JOURNAL OF SOLID STATE CHEMISTRY 79, 86–98 (1989)

A Study of the Ordering of Oxygen Vacancies in the Rare-Earth Perovskites $Sr_2MFe_3O_{8+y}$ by Mössbauer Spectroscopy

P. D. BATTLE, T. C. GIBB,* AND S. NIXON

Department of Inorganic and Structural Chemistry, The University, Leeds LS2 9JT, England

Received July 26, 1988

A large range of materials of general composition $Sr_2MFe_3O_{8+y}$ has been prepared for M = La, Ce, Pr, Nd, Sm, Eu, Gd, Dy, Er, Yb, and Y under a variety of conditions and studied by X-ray powder diffraction and Mössbauer spectroscopy. The nature of the product is affected to a surprising degree by the choice of M. The tendency to oxidation decreases rapidly across the series. The fully reduced phase ($y = 0$) is either cubic or orthorhombic. The high-temperature cubic phase is believed to have a macroscopic perovskite structure in which oxygen vacancies are partially ordered into alternate FeO_2 layers to form a coherent intergrowth of microdomains. Magnetic coherence pertains throughout the lattice. This phase is thermodynamically unstable at low temperatures with respect to the orthorhombic phase with vacancies ordered into every third layer, but for kinetic reasons the latter is not always achieved. Rapid oxidation during cooling takes place initially along microdomain boundaries.

Introduction

A major investigation in our laboratory into nonstoichiometry and defect ordering in the perovskite $Sr_2LaFe_3O_{8+y}$ has yielded interesting results (*1, 2*). In the composition range $0.6 < y < 1$ the material is a cubic perovskite at room temperature, and the Fe cations are all electronically equivalent in an averaged-valence state (*1*). At ca. 200 K there is a first-order transition to a low-temperature antiferromagnetic mixed-valence state by the nominal charge disproportionation

$$2Fe^{4+} \rightleftharpoons Fe^{3+} + Fe^{5+}.$$

Mössbauer spectroscopic data revealed that an increase in the oxygen vacancy concentration (decreasing y) depresses the transition temperature by some 50 K, and causes a degree of relaxational collapse in the magnetic hyperfine patterns. There is also some evidence for electron trapping in the vicinity of oxygen vacancies in the averaged-valence state. For $y < 0.6$ evidence was found for two new ordered vacancy phases (*2*). Orthorhombic $Sr_2LaFe_3O_8$ is an antiferromagnet (T_N = 715 ± 5 K), and is analogous to $Ca_2LaFe_3O_8$ (*3, 4*). Both compounds are believed to contain layers of iron cations in tetrahedral coordination, each separated by two layers in octahedral coordination to oxygen. Mössbauer data also revealed (*2*) the existence of a further "tetragonal" phase which appears to have a range of stoichiometry below the ideal composition of $Sr_2LaFe_3O_{8.5}$ and orders antiferromagnetically at about 500 K. The composition range $0 < y < 0.6$ could be explained in terms of varying amounts of

* To whom correspondence should be addressed.

0022-4596/89 $3.00

the orthorhombic and "tetragonal" phases. However, evidence was obtained for microdomain formation and intergrowth which suggests that it may not be strictly correct to regard all materials as simply a two-phase mixture.

A series of experiments was initiated to verify the expected similar behavior for compounds containing other rare-earth elements. This revealed new features in the defect ordering which are the subject of the present paper.

Experimental

Accurately weighed amounts of spectroscopic-grade Fe_2O_3, $SrCO_3$, and the appropriate rare-earth oxide, M_2O_3, with stoichiometric ratios appropriate for $Sr_2MFe_3O_8$ were ground together in a ball mill, pressed into a pellet, and initially fired in a platinum crucible at 1300°C (La 1400°C) for 4–7 days with two intermediate grindings before quenching onto a metal plate in air. Aliquots of this material were then treated in several different ways: annealing in air at 1300°C for about 3 days before quenching in air or into liquid nitrogen, or slow cooling in air to room temperature; annealing in argon for 3 days at 1200°C before slowly cooling at 50°C per hour to room temperature; annealing *in vacuo* (10^{-4} Torr) at various temperatures. Initial characterization in each case was by X-ray powder diffraction recorded with a Philips diffractometer using nickel-filtered Cu$K\alpha$ radiation. Chemical analyses for nominal Fe^{4+} content were carried out by digestion in a standardized solution of ammonium iron(II) sulfate in the presence of HCl and titration with cerium(IV) sulfate using ferroin as indicator.

^{57}Fe Mössbauer data were collected in the temperature range $4.2 < T < 773$ K using a ^{57}Co/Rh source matrix held at room temperature; isomer shifts were determined relative to the spectrum of metallic iron. ^{151}Eu data were obtained at 290 K using a source of ^{151}Sm/SmF_3; isomer shifts were determined relative to the source.

Results

A representative selection of the rare earths (and yttrium) were used to establish the effects of decreasing cation size on the defect properties (M = La, Ce, Pr, Nd, Sm, Eu, Gd, Dy, Y, Er, Yb). The initial synthesis was carried out at 1400°C for La, but the temperature was reduced to 1300°C for the others once it became evident that the yttrium preparation melted below 1400°C. Aliquots were then annealed in several different ways.

Samples Slowly Cooled in Air

Preparations of $Sr_2MFe_3O_{8+y}$ (M = La, Sm, Eu, Y, and Yb) were made by cooling slowly in air from 1300°C to encourage maximum oxidation. The oxygen parameters and X-ray characterization are given in Table I. The oxygen uptake in the case of lanthanum has been shown (*1, 2*) to vary smoothly as a function of temperature, and oxidation takes place continuously down to 400°C, being very rapid at the higher temperatures. As the ionic radius of M decreases across the rare-earth series (yttrium is taken to be similar in size to holmium), there is a very substantial decrease in the oxygen uptake which was

TABLE I

THE OXYGEN PARAMETER y AND X-RAY LATTICE PARAMETER a FOR SAMPLES OF $Sr_2MFe_3O_{8+y}$ COOLED SLOWLY IN AIR

M	y	a (Å)
La	0.94	3.874 (broad)
Sm	0.67	3.865 (very sharp)
Eu	0.41	3.866 (very sharp)
Y	0.31	3.866 (very sharp)
Yb	0.17	(cubic + ?)

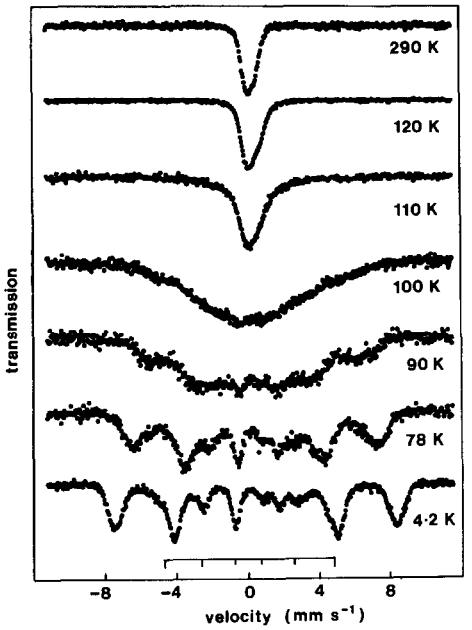

FIG. 1. The Mössbauer spectrum as a function of temperature for $Sr_2SmFe_3O_{8.67}$ slow-cooled in air from 1300°C.

achieved by cooling in air at atmospheric pressure. The Sm, Eu, and Y compounds gave very sharp cubic X-ray patterns. Yb was the exception in that the pattern appeared to be based on the cubic perovskite but with a number of weaker lines implying a larger perovskite-related cell of lower symmetry. However, we formed the opinion that the pattern was really a superposition of a cubic pattern upon that of a supercell, indicating either mixed phases or possibly a microdomain intergrowth.

The Mössbauer data were more informative. The spectra for La have already been described and interpreted in detail (*1*). $Sr_2LaFe_3O_{8.94}$ gave a single line resonance at 290 K because of a fast electron transfer which rendered all Fe cations equivalent within the time scale of the measurement (10^{-7} sec). Below 200 K the spectrum comprises two magnetic hyperfine sextets with flux densities at 78 K of 45.1 and 25.9 Tesla. There is no detectable quadrupole splitting, and the isomer shifts are +0.352 and −0.027 mm sec^{-1}, respectively. This data can be interpreted in terms of a charge disproportionation into species approximating to Fe^{3+} and Fe^{5+}. There is a first-order transition between the low-temperature mixed-valence state and the high-temperature averaged-valence state, although the two forms coexist over a wide temperature range (200–225 K). Reducing the oxygen content to $y = 0.69$ lowers the transition temperature by some 50° to ca. 170 K and causes a degree of relaxational collapse in the Mössbauer spectrum above 78 K. At the same time the spectra of the averaged-valence state become asymmetric, which is believed to indicate electron trapping in the vicinity of oxygen vacancies.

Similar series of spectra for $Sr_2SmFe_3O_{8.67}$ and $Sr_2EuFe_3O_{8.41}$ are shown in Figs. 1 and 2, respectively. In both cases

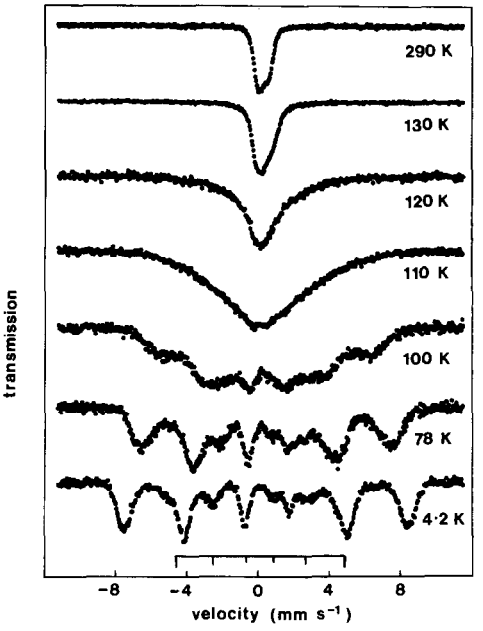

FIG. 2. The Mössbauer spectrum as a function of temperature for $Sr_2EuFe_3O_{8.41}$ slow-cooled in air from 1300°C.

measurements were made at 4.2 K to observe the static spectrum without relaxation effects. It can be seen that relaxation is already evident at 78 K, and the Sm system has completely transformed to the averaged-valence state at 120 K. The Eu system behaves in a similar manner, and the flux densities (49.3 and 28.1 T) and corresponding isomer shifts (0.43 and 0.05 mm sec^{-1}) at 4.2 K are in the range typical of cations approximating to Fe^{3+} and Fe^{5+}. The existence of this averaged valence phase at a much higher oxygen deficiency than could be obtained for La is interesting, although this may reflect the relative stability with respect to the other oxygen deficient structures we have found. The decrease in the transition temperature from La to Sm for a similar oxygen content is compatible with an increased Fe–O orbital overlap in the significantly smaller unit cell.

Although $Sr_2YFe_3O_{8.31}$ was also cubic to X-rays, the Mössbauer spectra (Fig. 3) reveal a very different situation. The material is now magnetically ordered at 290 K, and the paramagnetic averaged-valence phase appears not to exist, at least under ambient pressures, nor is it easy to determine the oxidation states of the Fe cations from the spectra because of the gross broadening and asymmetric line shapes. The Yb preparation also shows a broad magnetic pattern at 290 K.

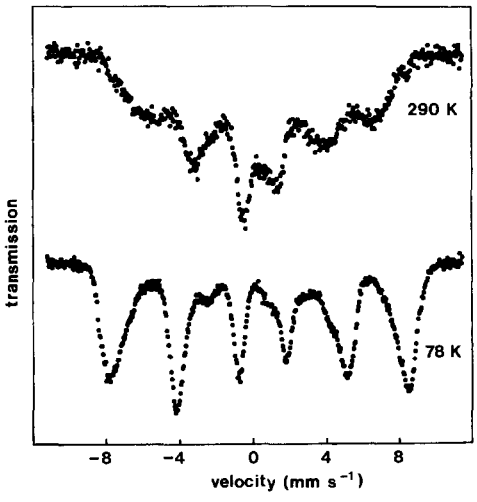

FIG. 3. The Mössbauer spectrum at 78 and 290 K of $Sr_2YFe_3O_{8.31}$ slow-cooled in air from 1300°C.

One may conclude that for materials prepared in air the degree of oxidation decreases across the rare-earth series, such that the averaged-valence phase becomes progressively more oxygen deficient and is eventually replaced by a magnetically ordered phase with localized electron states.

Samples Quenched in Liquid Nitrogen

Preparations of $Sr_2MFe_3O_{8+y}$ (M = La, Ce, Pr, Nd, Sm, Eu, Gd, Dy, Y, Er, and Yb) were made by annealing at 1300°C (La 1400°C) and quenching in liquid nitrogen. Lanthanum gave an apparent mixture of the orthorhombic and "tetragonal" phases (*2*). For M = Ce, Pr, Nd, Sm, Eu, Gd, Dy, and Y the product was shown by X-ray diffraction to be a simple cubic perovskite with very sharp diffraction lines. There is however a very diffuse reflection at a d-spacing of ~5.5 Å which we attribute to short-range ordering of the Sr/M cations. Only for Ce was there any suggestion of a small amount of a second phase. The oxygen and lattice parameters are given in Table II. For M = Er and Yb the X-ray pattern showed additional lines, suggesting the presence of a new phase with a larger unit cell (which was not identified) in addition to the stronger cubic pattern.

The oxygen parameter and X-ray lattice parameter decrease with decreasing size of the M cation. The Mössbauer spectra at 290 K for all eight cubic phases were basically the same and comprised a magnetic hyperfine pattern from presumed antiferromagetic ordering. The spectrum for $Sr_2EuFe_3O_{8.08}$ is shown in Fig. 4a as a typical example. The outside line on the right (more positive velocity) was always distinctly different in shape from the corre-

TABLE II

THE OXYGEN PARAMETER y AND X-RAY LATTICE PARAMETER a FOR SAMPLES OF $Sr_2MFe_3O_{8+y}$ QUENCHED INTO LIQUID NITROGEN FROM 1300°C

M	y	a (Å)
Ce	0.29	3.901
Pr	0.11	3.898
Nd	0.10	3.893
Sm	0.10	3.887
Eu	0.08	3.885
Gd	0.08	3.884
Dy	0.06	3.876
Y	0.06	3.872
Er	0.04	—
Yb	0.08	—

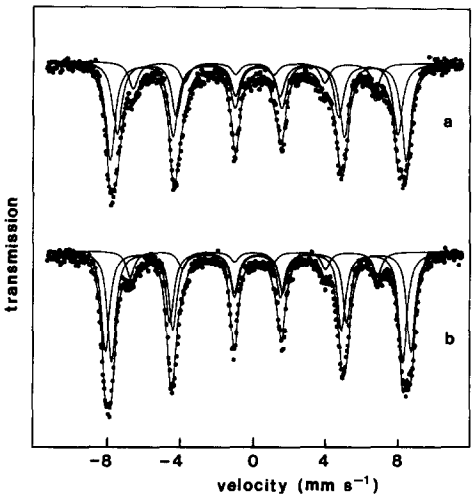

FIG. 4. The Mössbauer spectra at 290 K of (a) $Sr_2EuFe_3O_{8.08}$ quenched in liquid nitrogen from 1300°C and (b) $Sr_2EuFe_3O_{8.00}$ slow-cooled under argon from 1200°C.

sponding line on the left, and there was clear evidence of other weak components. It proved possible to analyze all eight spectra successfully using a comparatively simple model with three hyperfine fields (with flux densities B_1, B_2, and B_3), constrained to the same linewidth, and with no quadrupole perturbations. The theoretical fit for Eu is shown in Fig. 4a. The computed parameters are given in Table III. There was no conclusive evidence for an oxidation state of iron greater than +3 despite the small oxygen excess, although such a contribution could easily be hidden in the background.

The flux density B_3 and the isomer shift δ_3 are systematically lower than the other values, and we can assign this component with some degree of confidence to Fe^{3+} cations in 4-coordination. The isomer shifts δ_1 and δ_2 are distinctly different, as are the flux

TABLE III

THE MÖSSBAUER PARAMETERS AT 290 K FOR THE $Sr_2MFe_3O_{8+y}$ CUBIC PHASES QUENCHED FROM 1300°C INTO LIQUID NITROGEN

M	Γ (mm sec^{-1})	B_1 (T)	δ_1 (mm sec^{-1})	%	B_2 (T)	δ_2 (mm sec^{-1})	%	B_3 (T)	δ_3 (mm sec^{-1})	%
Ce	0.54	51.4	0.36	54	48.3	0.30	37	42.5	0.18	9
Pr	0.69	49.3	0.34	55	46.4	0.30	32	40.8	0.21	13
Nd	0.72	49.3	0.34	60	46.1	0.30	27	40.5	0.17	13
Sm	0.68	50.2	0.34	51	47.4	0.31	35	41.1	0.18	14
Eu	0.61	50.5	0.35	50	47.9	0.30	37	41.3	0.13	13
Gd	0.63	50.0	0.35	46	47.3	0.30	40	40.7	0.16	14
Dy	0.68	50.0	0.33	50	47.3	0.29	37	41.0	0.18	13
Y	0.63	50.2	0.34	55	47.5	0.31	34	41.0	0.14	11

densities, although the values for the latter are more susceptible to error because the intensities of the two components are strongly interactive in the computer fit. The analysis for the Ce compound is significantly different from the others. In general we feel that, due to the accessibility of the Ce^{4+} state, Ce may introduce new features which are not readily identifiable, and we prefer to exclude it from the discussion.

The average percentage of component 3 in the remaining seven compounds is 13%. The computed binomial probabilities for 6-, 5-, and 4-coordination in $Sr_2MFe_3O_8$ (with one in nine oxygen sites vacant) are 49, 37, and 12%. These figures are reasonably close to the computed values for the three components, and we conclude that sites 1, 2, and 3 derive from 6-, 5-, and 4-coordinate Fe^{3+} cations in a perovskite matrix with a close to random distribution of oxygen vacancies. The electric field gradient tensor at any given iron site will have a varying orientation with respect to the spin axis. The result is a large distribution of hyperfine patterns with small quadrupole perturbations which appear overall as a single broadened hyperfine pattern with a quadrupole perturbation of apparently zero. This point will be reemphasized below in connection with the argon-cooled samples. The Er and Yb samples gave spectra very similar to the others, implying that the bulk of the samples may be structurally similar to the simple cubic phases.

Samples Annealed under Argon

Preparations of $Sr_2MFe_3O_{8+y}$ (M = Ce, Pr, Nd, Sm, Eu, Gd, Dy, Er, and Yb) were annealed at 1200°C under argon before cooling slowly to room temperature. Although La produces an orthorhombic phase under these conditions (*2*), Ce, Pr, Nd, Sm, Eu, and Gd all gave a cubic perovskite with no other phase present. The lattice parameters are given in Table IV. The oxygen parameter y is small in all cases. However, the analysis relies on a back titration and blank calibration, so that the cumulative error in the values for small y is large. Although some samples were clearly a deep reddish brown, the color was often nearer to black (even for samples heated in high vacuum). Nevertheless, the excess oxygen content is believed to be small. The Mössbauer spectra and X-ray patterns for Pr, Nd, Sm, Eu, and Gd were all very similar, Ce again being noticeably different. The Mössbauer spectrum at 290 K for Eu is shown in Fig. 4b. It is very similar to that of the nitrogen quench in Fig. 4a, the main difference being a smaller linewidth which was general to all five cubic phases which were prepared under both conditions, and a nominally higher intensity for component 2 (see Table V) which is potentially an artifact of the computer fit. The Ce sample gave a sharper Mössbauer spectrum with less resolved evidence for the 4-coordinate site, and the data are omitted from the table as being unreliable.

The Eu sample was investigated in more detail. The Mössbauer spectrum as a function of temperature was measured in an evacuated furnace and shows a typical Bril-

TABLE IV

THE OXYGEN PARAMETER y AND X-RAY LATTICE PARAMETERS FOR SAMPLES OF $Sr_2MFe_3O_{8+y}$ ANNEALED UNDER ARGON AT 1200°C

M	y	a (Å)	b (Å)	c (Å)	V (Å^3)
La	0.08	5.514	11.901	5.606	367.9
Ce	0.25	3.899	—	—	(355.6)
Pr	0.05	3.900	—	—	(355.9)
Nd	0.05	3.896	—	—	(354.8)
Sm	0.01	3.889	—	—	(352.9)
Eu	0	3.885	—	—	(351.8)
Gd	0.08	3.884	—	—	(351.6)
Dy	0.03	5.485	11.657	5.550	354.9
Y	0.03	5.489	11.662	5.560	355.9
Er	0.05	5.477	11.600	5.550	352.6
Yb	0.03	5.473	11.584	5.556	352.3

TABLE V

THE MOSSSBAUER PARAMETERS AT 290 K FOR THE $Sr_2MFe_3O_{8+y}$ CUBIC PHASES ANNEALED UNDER ARGON AT 1200°C

M	Γ (mm sec^{-1})	B_1 (T)	δ_1 (mm sec^{-1})	%	B_2 (T)	δ_2 (mm sec^{-1})	%	B_3 (T)	δ_3 (mm sec^{-1})	%
Pr	0.57	50.6	0.36	47	48.0	0.31	40	41.2	0.16	13
Nd	0.57	50.8	0.35	49	48.2	0.31	38	41.7	0.14	13
Sm	0.59	52.1	0.37	42	49.6	0.30	47	42.2	0.11	11
Eu	0.54	52.1	0.36	42	49.7	0.30	47	42.1	0.11	11
Gd	0.65	49.3	0.33	51	46.7	0.29	33	40.4	0.19	16

louin collapse with an ordering temperature of ca. 760 K (Fig. 5). The three hyperfine fields are not well resolved at the higher temperatures, and no analysis was attempted. At 773 K, the compound is paramagnetic, and the Mössbauer spectrum shows a clearly resolved quadrupole splitting of 0.81 mm sec^{-1}, although the large linewidth of 0.57 mm sec^{-1} suggests that there may be a distribution of quadrupole splittings rather than a single value. A quadrupole splitting is not seen in the magnetic spectra because of a larger number of orientations with respect to the spin axis as already explained for the nitrogen quenched samples.

The Dy, Y, Er, and Yb samples are entirely different. The X-ray patterns can be indexed on the basis of the same orthorhombic cell as $Sr_2LaFe_3O_8$. However, the lines are broader suggesting a more disordered material. The cell parameters are given in Table IV, together with the cell volume V. Also shown is the appropriately normalized cell volume for the cubic phases, and it can be seen that the orthorhombic cell has a markedly larger volume than that which would be predicted by extrapolation from the cubic phase. The Mössbauer spectra at 290 K are shown in Fig. 6, and the relevant parameters in Table VI. There are two magnetic hyperfine sextets from the octahedral and tetrahedral sites, although the linewidths of the latter are uniformly larger. The ideal area ratio for the octahedral : tetrahedral sites is 2 : 1, and even allowing for different recoilless fractions there is a considerable deviation from this in the case of ytterbium. The Mössbauer spectra and X-ray lines are both broadened compared to the other elements, and the ordering of the oxygen vacancies is probably less advanced in this sample.

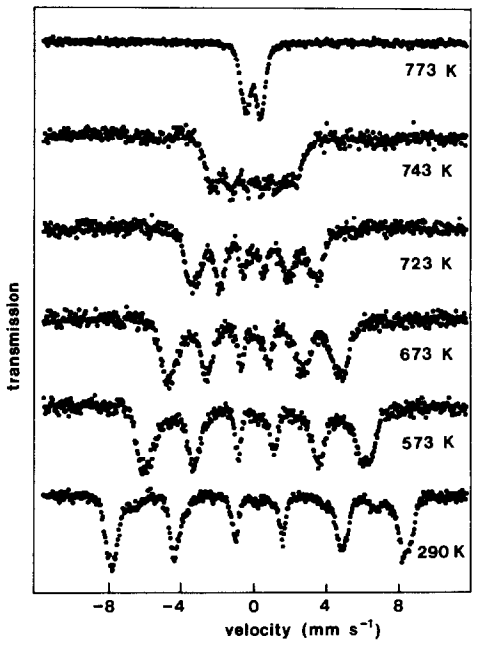

FIG. 5. The Mössbauer spectrum as a function of temperature for $Sr_2EuFe_3O_8$ slow-cooled in argon from 1200°C.

TABLE VI

THE MÖSSBAUER PARAMETERS AT 290 K FOR THE ORTHORHOMBIC $Sr_2MFe_3O_8$ PHASES ANNEALED AT 1200°C AND COOLED IN ARGON

M	B_O (T)	δ_O (mm sec^{-1})	ε_O (mm sec^{-1})	B_T (T)	δ_T (mm sec^{-1})	ε_T (mm sec^{-1})	$\%_T$
La	51.5	0.35	−0.20	38.0	0.19	+0.36	35
Dy	50.9	0.33	−0.19	38.1	0.19	+0.29	31
Y	51.5	0.34	−0.17	37.5	0.17	+0.39	27
Er	51.3	0.33	−0.17	37.3	0.17	+0.36	33
Yb	51.3	0.33	−0.14	38.1	0.15	+0.38	19

Note. The parameters refer to the octahedral (O) and tetrahedral (T) sites.

Samples Annealed in Vacuo

A sample of $Sr_2LaFe_3O_8$ of good quality was achieved in our earlier work (*2*) by annealing *in vacuo* at 1000°C. More recently a repeat of this preparation was carried out at 1000°C with a continued anneal at 800°C to give the orthorhombic phase. This was then followed by a second anneal at 1100°C for 8 days and 800°C for 6 days. Surprisingly the product proved to be completely different. The X-ray pattern was at first sight a simple cubic perovskite with $a_p = 3.920$ Å in agreement with the other cubic phases, but there were also a number of broad weak superlattice lines which could be indexed on the basis of a tetragonal cell $a_p \times a_p \times 2a_p$, i.e., doubled along one cell edge. The Mössbauer spectrum (Fig. 7) at 290 K was also considerably different. The spectrum is not symmetrical because of quadrupole perturbations, and there is clear evidence for at least three hyperfine patterns. A computer analysis fitting three such patterns was not entirely convincing because of asymmetry in the line shapes, but the parameters ob-

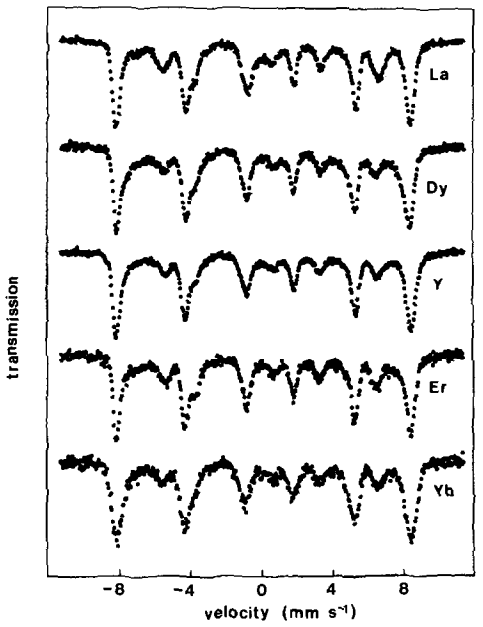

FIG. 6. The Mössbauer spectra at 290 K for five orthorhombic phases obtained by cooling from 1200°C under argon.

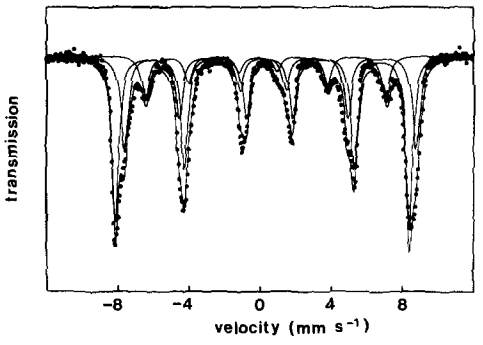

FIG. 7. The Mössbauer spectrum at 290 K of $Sr_2LaFe_3O_8$ annealed *in vacuo* at 1100°C. An attempted analysis in terms of three hyperfine fields is shown.

TABLE VII

THE MÖSSBAUER PARAMETERS AT 290 K FOR $Sr_2LaFe_3O_8$ WITH A PEROVSKITE CELL DOUBLED ALONG ONE CELL EDGE

Site	B (T)	δ (mm sec^{-1})	ε (mm sec^{-1})	%
1	51.4	0.33	−0.19	51
2	51.0	0.39	+0.20	32
3	42.0	0.14	+0.20	17

tained (Table VII) give a close representation of the behavior. All three sites show a significant quadrupole perturbation. Site 1 comprises some 51% of the spectrum and gives parameters very close to those shown by the octahedral sites in orthorhombic $Sr_2LaFe_3O_8$. Site 3 comprises about 17% of the spectrum and shows the flux density and isomer shift normally associated with tetrahedral sites, although the percentage is much lower than the 33% expected for the orthorhombic phase. Site 2 shows a similar flux density to site 1, but with a quadrupole perturbation of opposite sign. This can be tentatively assigned to sites in 5-coordination. However, it is likely that this model is too naive, and that either there are more than three distinct iron sites, or that there is a range of local environments. Nevertheless, this sample represents the *fourth* distinct structural phase that we have found in the $Sr_2LaFe_3O_{8+y}$ system.

A further anneal at 1000°C for 3 days restored the orthorhombic phase once more, and one can deduce that the system is kinetically inert at 800°C, the difference in the product being determined by the higher temperature. The sample was then annealed at 1300°C *in vacuo* for 3 days and then quenched quickly by removing from the furnace. The X-ray pattern was still that of the orthorhombic phase again, with no apparent evidence for any of the cubic phase. The weak diffuse absorption at a d-spacing of ~5.5 Å associated with Sr/La short-range ordering was very weak, but otherwise the spectrum was the same as recorded for the anneal at 1000°C.

A sample of $Sr_2NdFe_3O_8$ was prepared by annealing at 1000°C *in vacuo* for 3 days. The X-ray pattern remained that of a cubic perovskite, apart from the diffuse feature at $d \simeq 5.5$ Å from Sr/La short-range order. There was no evidence for ordering of the oxygen vacancies.

Samples Quenched in Air

Although the samples were usually quenched in air during the initial firings, considerable oxidation takes place during the quench and the nature of these materials was not investigated fully in all cases. The sample of $Sr_2LaFe_3O_{8.336}$ quenched in air from 1400°C was described earlier (*2*), and some evidence was found to suggest that the quench produces a microdomain texture and intergrowth of $Sr_2LaFe_3O_8$ and the "tetragonal" phase. A sample of $Sr_2SmFe_3O_{8.223}$ quenched from 1300°C gave a broadened cubic X-ray pattern, and the Mössbauer spectra are shown in Fig. 8. The temperature dependence of the latter shows the same features that we reported earlier in Sr_2FeCoO_{5+y} and $Ca_2LaFe_3O_{8+y}$ quenched in air (*5, 6*) and interpreted in terms of microdomain formation. At 78 K the spectrum is similar to that of the nitrogen-quenched cubic phase apart from a subtle broad curvature to the background. With increase in temperature a new central component appears which grows at the expense of the magnetic pattern. The isomer shift of this central feature is more positive than that of the averaged-valence phase, and the possibility of a two-phase mixture can be excluded. The rapid oxidation which takes place during the quench results in the formation of small microdomains of the original cubic phase, with the oxygen excess incorporated in the domain walls. These domains behave in a similar manner to superparamagnetic particles so that the

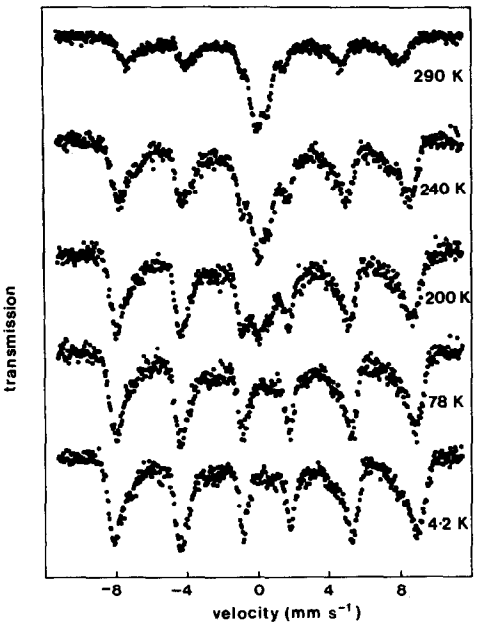

FIG. 8. The Mössbauer spectrum as a function of temperature for $Sr_2SmFe_3O_{8.223}$ quenched in air from 1300°C.

spin axis relaxes more quickly in the smaller domains and produces the spectral collapse seen in Fig. 8. A full explanation of these effects has already been given (*5*, *6*).

Similar data were obtained for $Sr_2EuFe_3O_{8.196}$, but the collapse does not develop until a noticeably higher temperature. This is consistent with the existence of larger microdomains in a less-oxidized matrix.

^{151}*Eu Mössbauer Spectra*

The existence of a second convenient Mössbauer isotope (^{151}Eu) in the four europium samples enabled us to obtain additional information. In previous studies of the orthoferrites and their solid solutions (*7–9*) it was found that the linewidth of the ^{151}Eu resonance can be broadened by unresolved hyperfine effects. For example, the linewidth of $EuFeO_3$ was observed to be 3.27 mm sec^{-1} compared to only 2.26 mm sec^{-1} in hydrated europium nitrate, and this broadening was shown to be the result of a quadrupole interaction. Magnetic hyperfine splitting can be produced by a transferred magnetic exchange interaction as seen, for example, in Sr_2EuRuO_6 and $Sr_2Eu_2Fe_2O_7$ (*10*, *11*), but the effect is negligible in $EuFeO_3$ because pairs of iron atoms in the antiferromagnetic structure cause mutual cancellation. However, in solid solutions such as $EuFeO_3$–$EuCoO_3$ and $EuFeO_3$–$EuCrO_3$ the replacement of iron by cobalt or chromium can cause a small asymmetry in the interaction and a resultant molecular exchange field at the Eu nucleus which leads to a linewidth of up to 7 mm sec^{-1}.

The ^{151}Eu Mössbauer spectra for the four $Sr_2EuFe_3O_{8+y}$ samples are shown in Fig. 9, and the parameters are given in Table VIII. The sample slow-cooled in air has the smallest linewidth; it is also the only sample

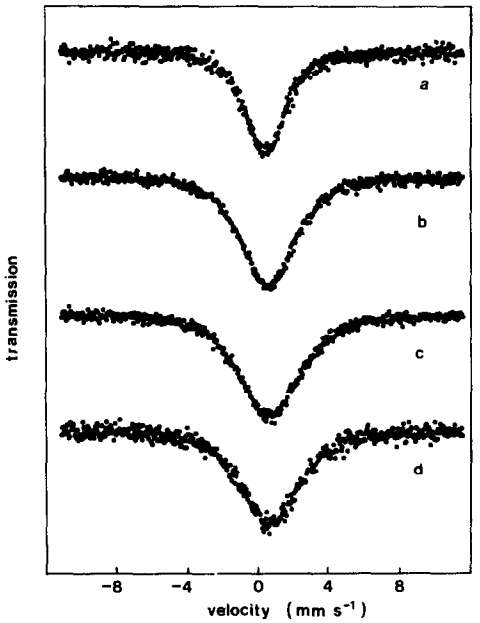

FIG. 9. The ^{151}Eu Mössbauer spectra of $Sr_2EuFe_3O_{8+y}$ (a) slow-cooled in air, (b) quenched in air, (c) quenched in nitrogen, and (d) slow-cooled in argon.

TABLE VIII

THE ^{151}Eu MÖSSBAUER PARAMETERS AT 290 K

Sample	y	δ	Γ
Slow cool in air	0.41	0.28	2.60
Quench in air	0.20	0.45	3.51
Quench in N_2	0.08	0.52	4.06
Slow cool in argon	0	0.53	3.89

to be in the paramagnetic state at room temperature. Any quadrupole interaction is small. The larger linewidths in the three magnetic samples may therefore be due to the small asymmetry in the molecular exchange field caused by the influence of oxygen vacancies. Up to one in nine of the oxygen sites are vacant, which is significant in terms of the normal 12-coordination to oxygen of Eu in a cubic perovskite. A further observation is the increase in isomer shift upon reduction and loss of oxygen, which is indicative of an increase in electron density as the coordination number is reduced.

Unfortunately there is no suggestion of any resolution of different Eu environments, and the observed spectra can only be considered in general terms as a weighted average.

Discussion

The major contribution of this paper is in the characterization of oxygen deficient compounds close to the composition $Sr_2MFe_3O_8$ which are prepared at high temperatures. These results are highly relevant to the more general study of cubic perovskites with a high concentration of oxygen vacancies.

The reduced $Sr_2Fe_2O_5$–$MFeO_3$ solid solution (and the $Sr_2MFe_3O_8$ composition in particular) has largely escaped attention. Some time ago a study of the reduced system $Sr_{1-x}La_xFeO_{(5+x)/2}$ made reference (*12*) to a cubic perovskite phase for $x = 0.3$, 0.4, 0.5, and 0.6. Unfortunately the Mössbauer data are of poor quality by current standards, but the magnetic hyperfine patterns do demonstrate that the number of tetrahedral sites is substantially reduced in favor of presumed 5-coordinate sites. Interestingly, the samples were quenched *in vacuo* at 1100°C, which was the temperature at which we obtained the doubled perovskite cell.

Very few data are available for the later rare earths. There is an interesting reference to $Sr_{0.8}Nd_{0.2}FeO_{2.60}$ annealed in argon at 1350°C and cubic to X-ray diffraction (*13*). Electron diffraction, which uses a shorter wavelength, showed evidence for a doubling of one of the perovskite cell axes at random in the *a*, *b*, and *c* directions. Electron micrographs showed a random intergrowth of small microdomains, and it was tentatively suggested that tetrahedral sites are ordered into alternate layers.

A paper published on $Sr_{1-x}Dy_xFeO_{3-y}$ while this work was in progress (*14*) refers only to material quenched in air from 1200°C (the nearest relevant composition being $x = 0.25$). From our own work this is likely to produce very inhomogeneous nonequilibrium microdomain materials, and there are insufficient data to add to our interpretation. We have concentrated on the $Sr_2MFe_3O_{8+y}$ system because this composition is appropriate to the formation of an ordered orthorhombic phase. However, the system is not considered to be a line phase, and similar behavior can be expected at slightly different Sr/M ratios.

It is especially important to be aware that the phases obtained at room temperature by rapid quenching are not necessarily those which existed in equilibrium before the quench. This is clearly demonstrated by the related compound $Sr_2Fe_2O_5$ (or $SrFeO_{2.5}$) which has the orthorhombic brownmillerite structure and alternate layers of iron in octahedral and tetrahedral coordination. It has been shown to undergo a transition to a cubic phase above ~850°C (*15*), but it is

apparently not possible to preserve the cubic phase by very fast quenching. Furthermore, it has recently been shown (*16*) by Mössbauer spectroscopy that the distorted local site symmetries of the brownmillerite structure are retained by most of the iron atoms for some 200°C above the transition temperature before diffusion of the oxygen vacancies causes any significant motional narrowing effects. This provides some evidence to support the postulate (*15*) that the high-temperature cubic phase contains a disordered intergrowth of microdomains of a near brownmillerite lattice in three orthogonal directions.

One very significant feature of all the cubic $Sr_2MFe_3O_8$ (i.e., $y = 0$) phases studied here is the lack of any relaxation behavior in the magnetic hyperfine spectrum. In the case of $Sr_2EuFe_3O_8$ this appears true right up to the ordering temperature of 760 K. This leads to the important conclusion that the Fe^{3+} spin interactions take place coherently over much larger distances than the ~200 Å resolution of X-ray diffraction. Since there is no evidence to suggest that the Sr^{2+} and M^{3+} cations can undergo any long-range order in these materials, one can assume that both cation lattices remain coherent over large distances, and that it is ordering of the oxygen vacancies which is responsible for the different structures.

A similar situation has been convincingly demonstrated (*17*) by electron micrographs for the phase $SrFe_{0.9}V_{0.1}O_{2.6}$ where the ordering of strings of oxygen vacancies along one or other of the six ⟨110⟩ directions of the cubic cell leads to the formation of microdomains of a superlattice which is a disordered variant of the brownmillerite structure, having a periodicity of $2a_p$. The high-resolution images show a good structural coherence of the cation sublattice throughout a particle despite the presence of many small microdomains. The excess oxygen tends to locate in the boundary regions.

This behavior is distinct from the magnetic properties of the microdomains found in $Ca_2LaFe_3O_{8+y}$ quenched in air (*6*), where there is no long-range spin coherence. Nevertheless, evidence for microdomain formation similar to that observed in the Ca compound has been found in the Sm and Eu systems in the present work. If microdomain boundaries already exist at high temperature they can provide a disordered pathway which is more susceptible to invasion by oxygen than the more ordered centers of the domains. It is then possible to combine the two types of microdomain into a unified model.

One of the biggest surprises in this work has been the stabilization of the cubic phase of $Sr_2MFe_3O_8$ at the expense of the orthorhombic phase which was only found for the largest and smallest cations. The observation of both phases for Dy and Y shows that the cubic phase is the high-temperature form. Although oxidation of $Sr_2LaFe_3O_8$ can take place down to ~400°C, we have found that at very low oxygen partial pressure the perovskite phase with a doubled unit cell is kinetically inert at 800°C. This leads us to believe that there may be a close competition between kinetic and thermodynamic factors which can prevent formation of the orthorhombic phase for some of the elements.

The observation of a doubled-cell perovskite in $Sr_2LaFe_3O_8$ annealed *in vacuo* at 1100°C rather than the expected orthorhombic phase may mean that a high-temperature form has been preserved here also. The observation of quadrupole perturbations in the Mössbauer spectrum is almost certainly a consequence of an increased degree of distortion in large ordered domains which is not possible in smaller microdomains. It appears to be the same defect structure already reported for $Sr_{0.8}Nd_{0.2}FeO_{2.60}$ (*13*). However, contrary to the earlier suggestions, the structure does not appear to contain a significantly

higher tetrahedral site concentration than in a random distribution of vacancies. Nevertheless, in compounds where the oxygen vacancy concentration is so high (1 : 6 in $Sr_2Fe_2O_5$, 1 : 9 in $Sr_2LaFe_3O_8$) it has been shown (*18*) that a completely random distribution of vacancies produces *A* cations (i.e., Sr) in unacceptably low coordinations. The ideal perovskite lattice can be described as alternating layers of stoichiometry SrO and FeO_2 perpendicular to $[100]_c$. It is numerically feasible to distribute the vacancies in $Sr_2LaFe_3O_8$ almost entirely in alternate FeO_2 layers without significantly increasing the number of 4-coordinate sites above that expected for a random distribution; there are fewer oxygen vacancies than in the brownmillerite case. The order over large distances in this particular preparation may have produced a greater resistance to transformation to the orthorhombic phase than was found for the quench from 1300°C where the equilibrium phase should be more disordered but still quenched as an orthorhombic phase.

The model which emerges to describe the high-temperature cubic phase is of a macroscopic perovskite lattice in which oxygen vacancies are partially ordered into alternate FeO_2 layers to form a coherent intergrowth of microdomains. Magnetic coherence persists throughout the lattice. This phase is thermodynamically unstable at lower temperatures with respect to the orthorhombic phase with vacancies ordered into every third FeO_2 layer, but for kinetic reasons this ordering is not always achieved. Additional oxygen can be incorporated, but in the case of $Sr_2LaFe_3O_{8+y}$ this results in a phase separation into $Sr_2LaFe_3O_8$ and "tetragonal" $Sr_2LaFe_3O_{8.5}$, analagous to the $Sr_2Fe_2O_5$ and $SrFeO_{2.75}$ case (*2*). Rapid oxidation of the other $Sr_2MFe_3O_8$ phases during cooling takes place along the microdomain boundaries to produce magnetically isolated microdomains of the cubic phase.

Acknowledgments

We thank the SERC for financial support and Mr. A. Hedley for the chemical analyses.

References

1. P. D. BATTLE, T. C. GIBB, AND S. NIXON, *J. Solid State Chem.* **77,** 124 (1988).
2. P. D. BATTLE, T. C. GIBB, AND S. NIXON, *J. Solid State Chem.* **79,** 75 (1989).
3. J. C. GRENIER, J. DARRIET, M. POUCHARD, AND P. HAGENMULLER, *Mater. Res. Bull.* **11,** 1219 (1976).
4. J. C. GRENIER, F. MENIL, M. POUCHARD, AND P. HAGENMULLER, *Mater. Res. Bull.* **12,** 79 (1977).
5. P. D. BATTLE, T. C. GIBB, AND S. NIXON, *J. Solid State Chem.* **74,** 60 (1988).
6. T. C. GIBB, *J. Solid State Chem.* **74,** 176 (1988).
7. T. C. GIBB, *J. Chem. Soc. Dalton Trans.*, 2245 (1981).
8. T. C. GIBB, *J. Chem. Soc. Dalton Trans.*, 873 (1983).
9. T. C. GIBB, *J. Chem. Soc. Dalton Trans.*, 2031 (1983).
10. T. C. GIBB AND R. GREATREX, *J. Solid State Chem.* **34,** 279 (1980).
11. T. C. GIBB, *J. Phys. C: Solid State Phys.* **14,** 1985 (1981).
12. H. YAMAMURA AND R. KIRIYAMA, *Bull. Chem. Soc. Japan* **45,** 2702(1972).
13. M. A. ALARIO-FRANCO, J. C. JOUBERT, AND J. P. LÉVY, *Mater. Res. Bull.* **17,** 733 (1982).
14. C. H. YO, E. S. LEE, AND M. S. PYON, *J. Solid State Chem.* **73,** 411 (1988).
15. J. C. GRENIER, N. EA, M. POUCHARD, AND P. HAGENMULLER, *J. Solid State Chem.* **58,** 243 (1985).
16. M. TAKANO, T. OKITA, N. NAKAYAMA, Y. BANDO, Y. TAKEDA, O. YAMAMOTO, AND J. B. GOODENOUGH, *J. Solid State Chem.* **73,** 140 (1988).
17. N. NAKAYAMA, M. TAKANO, S. INAMURA, N. NAKANISHO, AND K. KOSUGE, *J. Solid State Chem.* **71,** 403 (1987).
18. S. KOMARNICKI, J. C. GRENIER, M. POUCHARD, AND P. HAGENMULLER, *Nouv. J. Chem.* **5,** 161 (1981).